Geology, Geomorphology and Slope Instability of the Maar Lake Pavin (Auvergne, French Massif Central)

9

Jean-Claude Thouret, Pierre Boivin, Philippe Labazuy, and Alberic Leclerc

Abstract

Maars are craters created by violent phreatomagmatic eruptions. The crater shape involves roughly circular rims whose asymmetric slopes may be unstable long after the initial eruption. Lakes that occupy many maars are natural receptacles that enclose geologic archives such as slope deposits. Here we describe the geologic and geomorphic characteristics of the maar and Lake Pavin in Auvergne with emphasis on recent and current slope instability. This is due to its geometry (the 800 × 92 m lake occupies a wide depression cut deep in pre-existing lava flows and Montchal cone), loose surficial formations on steep subaerial slopes and fractured lava scarps, and loose and gas-rich sediment on sub-lacustrine steep slopes.

Our study of the outer rim slopes (<20°) of the maar shows that current geomorphic processes apparently act slowly, but mapping of the steepest (>31°), inner rim slopes suggests that instability is now related to runoff, *solifluction* and perhaps rockslides or deep-seated landslides. The slow and often small-sized mass movements occur on steep slopes >31° and fractured lava flow scarps while solifluction is favored by loose and thick, surficial maar deposits and a 4–5 month-long snow cover. Geomorphic anomalies on top of the north and NE maar rims suggest deep-seated, (slow moving?) rotational landslides that may record a long-lasting post-eruptive response to maar collapse. One of the large, recent rock fall scree on the NNE edge of the lake is apparently connected to the submerged platform capping a syn-eruptive collapse mass. The quasi-vertical edge of this platform may act as a source of debris transfer towards the deep lake bottom. Long subaerial slopes south and SE of the maar point out to the most unstable sector: fractured, thick lava flow scarps topple and produce scree, and permanent springs feed runoff and streams above the underlying clay-rich pyroclastic deposit. The south slope overhangs subaquatic lava cliffs which can transfer debris directly to the lake bottom 90 m below. In contrast, mapping of the recent fan of the lake outlet and the adjacent Gelat valley to the north, in which the outlet stream is incised, show no evidence for debris-flow deposits that were claimed to be emplaced by a historical catastrophic event triggered by a lake breakout.

Keywords

Lake Pavin • Maar • Slope • Instability • Lava • Pyroclastic deposit • Fan • Hazard

J.-C. Thouret (✉) • P. Boivin • P. Labazuy
LMV, Université Clermont-Auvergne - CNRS - IRD - OPGC, Aubière, France
e-mail: J.C.Thouret@opgc.univ-bpclermont.fr

A. Leclerc
Ecole Supérieure des Géomètres et Topographes, 1 Bd. Pythagore, 72000 Le Mans, France

9.1 Introduction

9.1.1 Maar, Landform and Process Definition

Hydrovolcanic landforms created by phreatomagmatic eruptions encompass tuff rings, tuff cones and maars. Like

T. Sime-Ngando et al. (eds.), *Lake Pavin*, DOI 10.1007/978-3-319-39961-4_9

calderas but smaller sized, maars are negative landforms excavated in the pre-eruption surface, in volcanic and non-volcanic bedrock. Unlike calderas maars characterize small-volume and short lived volcanoes commonly defined as monogenetic volcanoes with a central crater cut deeply into the pre-eruptive country rocks, surrounded by a low ring wall of pyroclastic material (tephra/tuff ring), and underlain by a diatreme (Ollier 1967; Lorenz 1973, 1986, 1987, 2007; Cas and Wright 1987; Vespermann and Schmincke 2000). Originally the term maar described a topographic feature, consisting of a crater and a tephra/tuff rim, but this term now incorporates the ring wall, the crater sediments, the diatreme and the feeder dyke. A maar is the crater cut into the ground below the syn-eruptive surface and surrounded by an ejecta ring, while the diatreme structure continues downward and encloses diatreme and root zone deposits (White and Ross 2011; Németh and Kereszturi 2015).

The syn-eruptive processes are driven by magma/groundwater, Molten Fuel-(Impure) Coolant explosive Interaction (MFCI) and produce mostly base *surge* and phreatomagmatic fallout beds up to a few tens of meters thick around the excavated maar crater (Wohletz 1986; Buettner et al. 2002; Lorenz 2007). During the post-eruptive processes subsequent to the formation of the maar basin, the intersection of the groundwater level leads to formation of a lake (Büchel and Lorenz 1993; Christenson et al. *in* Rouwet et al. 2015). The lake formation in the maar crater is usually a fast process but it depends on the permeability of the disrupted country rock, the geometry of the water storage system, and the availability of groundwater (Pirrung et al. 2008). The long-term sedimentary filling of the lake is controlled by (i) mass movements (mass flows of any type from the inner crater wall), (ii) delta deposits, (iii) atmospheric loads, mostly ash fall from nearby eruptive sites, (iv) production of organic matter in the lake, and (v) intensive mineral-rich spring activity (Pirrung et al. 2007, 2008; Németh et al. 2008; White and Ross 2011; Fox et al. 2015). Other processes can be called in for the relatively rapid sediment infill such as the post-eruptive subsidence of the maar, which may contribute to the maar lake deposit compaction and resettlement (Suhr et al. 2006; Lorenz 2007).

9.1.2 Scope and Objectives

We describe the geologic and geomorphic context of the maar and lake in order to examine potential factors of instability linked to both maar slopes and/or the lake outlet. The motivation of this study lies on the claim related to recent (post 6700 years) eruptive activity and Middle Ages catastrophic mudflow triggered by lake breakout subsequent to subaquatic landslide(s) (Lavina and Del Rosso-D'Hers 2008, 2009). This claim originated from geologic mapping of the area by the authors following earlier studies on volcanic lakes in Auvergne (e.g. Glangeaud 1916). As limnic eruptions occurred in crater lakes such as the lethal Lake Nyos event in Cameroon in 1986 (Lockwood et al. 1988; Tassi and Rouwet 2014), investigations have re-considered the volcanic lakes in Auvergne and Pavin in particular (Fig. 9.1). Camus et al. (1993) and more recently Olive and Boulègue (2004) concluded that despite its meromicticity, Lake Pavin does not present an imminent threat of violent CO_2 degassing due to lake overturn induced by a volcanic or limnic eruption. Meromicticiy defines lakes that have layers of water that do not intermix (Touchard 2000; Jézéquel et al. 2008; Rouwet et al. 2015). Various hydrothermal venues and carbogaseous springs as well as CO_2 emissions are known in the area at Escarot 3 km WSW and Fontaine Goyon 2 km ENE of Lake Pavin (Gal and Gadalia 2011; Fig. 9.1). The regionally known CO_2 has carbon isotope ratios that bind it to a magmatic origin from the upper mantle, linked to attenuation and fracturing of the continental crust beneath the Massif Central (Olive and Boulègue 2004; see also Alberic et al. 2013 for a more recent carbon reservoir analysis).

The objectives of the paper are twofold: (1) Link evidence of instability on the maar rims with subaquatic landforms such as the syn-eruptive, subaquatic platform mantled by sediment cover in the NNE sector of the lake described by Chapron et al. (2010a,b); (2) Unravel whether or not the fan created by the lake outlet can be related to recent events that have been postulated on the basis of historical landslide deposits dated from lake sediment (Fig. 9.1). Besides the geomorphological mapping of maar rims and the adjacent Couze Pavin Valley, we seek to detect geomorphic signs which may suggest current or recent instability above the lake shore. Slope instability may be related either to the steep maar rims (rock fall from lava flow scarp, slump and runoff in *tephra*) and to mass movements (subaquatic slumps and *turbidites*) that occurred in the recent past in the lake. Chapron et al. (2010a,b, 2012) have summarized natural hazards linked to a group of lakes in the French Massif Central and the Pavin maar lake in particular. Geophysical investigations, sedimentary cores and C^{14} ages have allowed the authors to reveal that landslides occurred twice inside the lake between AD 580–640 and as recently as AD 1200 and 1300. Lavina and Del Rosso-D'Hers (2009) and Del Rosso-D'Hers et al. (2009) claimed that debris-flow deposits they observed in the adjacent Gelat valley to the north resulted from the most recent of these events (see Sect. 9.4.4 below). We will report geomorphic indicators for current slope instability of the maar rims and we discuss the claim on debris-flow deposits related to the postulated lake breakout.

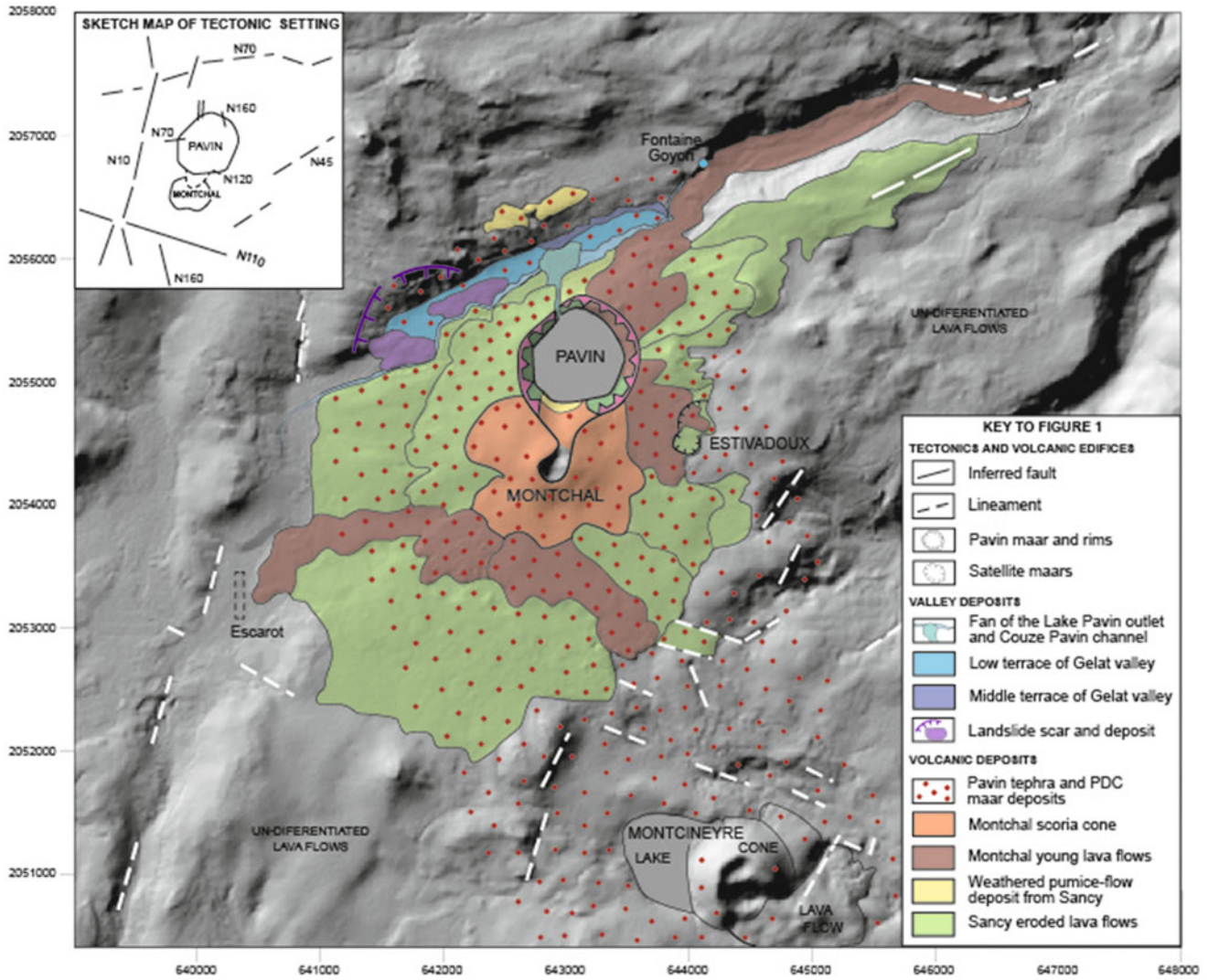

Fig. 9.1 Geologic setting of the Lake Pavin maar and surroundings. The area of carbogazeous springs and mofettes near Escarot and the CO_2-rich spring of La Fontaine Goyon are indicated

9.2 Study Site: Pavin Maar, Lake and Surroundings

Pavin is the only meromictic maar lake in France (Chaps. 1, 5 and 10, in this volume), which is surrounded by several older, small lakes of volcanic origin as shown in Chap. 23, Fig. 23.1. Lake Pavin (45° 55′ N; 2°54′ E) is located at 1197 m asl. in a remote area of the department of Puy-de-Dôme on the eastern slope of the Monts-Dore-Sancy strato-volcano in the French Massif Central. The almost circular lake has a diameter of about 800 m, a surface area of 44.5 ha and a maximum water depth of 92 m (Fig. 9.1). The Montchal lavas have then been partly removed by the Pavin phreatomagmatic eruption, first ^{14}C dated at 6900 ± 50 year ago (Gewelt and Juvigné 1988; Juvigné 1992a,b), but statistically revised as 6730 ± 130 years ago using new calibration curve and new data (Juvigné and Miallier; Chap. 8, in this volume). Primary deposits of eruption have been recognized on a large area around the lake (Bourdier 1980; Leyrit et al., Chap. 6, in this volume). This recent volcanic event formed Lake Pavin: a roughly circular and deep maar lake draining a steep and well preserved crater rim reaching an altitude of 1253 m asl. Nowadays, the maar rims wall rise, for the most part, 50–80 m above the lake surface but the maar intersects the north flank of the Montchal strombolian cone that rises as high as 210 m above the south lake edge (Figs. 9.1, 9.2, and 9.3).

As shown in Fig. 9.3, the edge of the Pavin maar tephra ring matches the limit of the topographic drainage basin of Lake Pavin except on the south flank of Montchal. It is however important to keep in mind that this topographic drainage basin is smaller than the still poorly defined watershed of Lake Pavin, approximately 2 km^2, draining several subaerial and subaquatic springs (Bonhomme et al. 2011). Pavin's

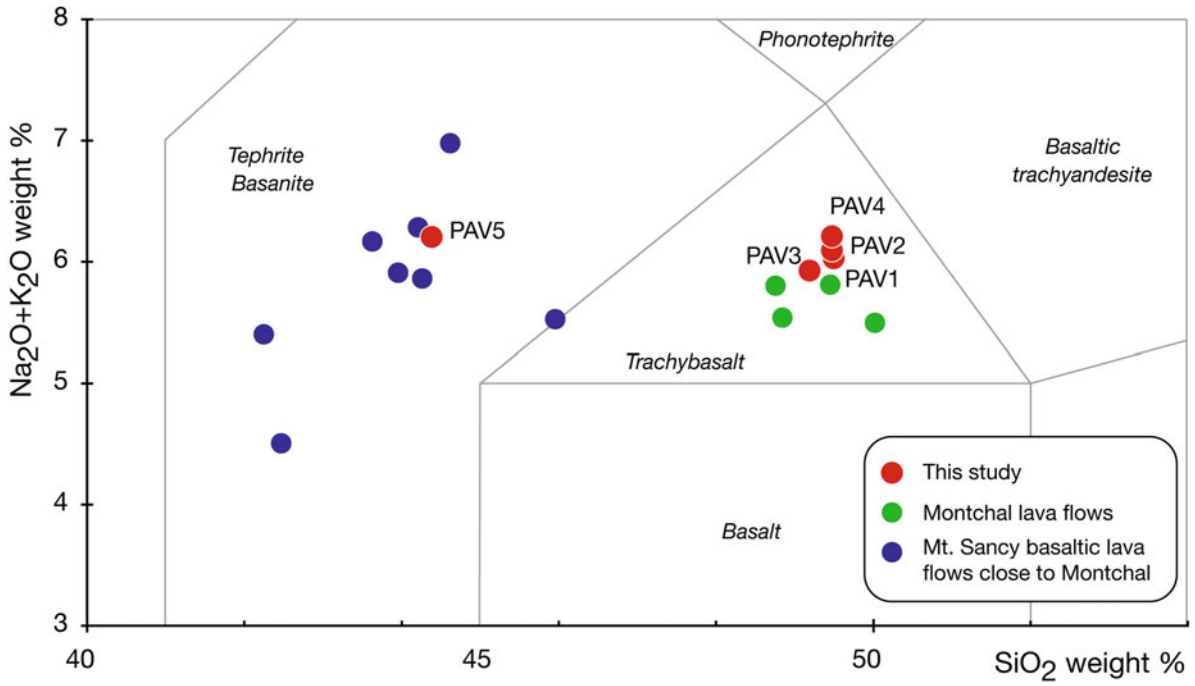

Fig. 9.2 TAS diagram showing five lava samples (no.1–5 *red* dots, located in Fig. 9.3) of the lava flows cut by the maar and surrounding the lake: one quasi-aphanitic tephrite sample (PAV5) with a few phenocrysts of leucite and olivine from the NE cliff, and four porphyritic trachybasalt samples (PAV1-4) with phenocrysts of olivine, clinopyroxene and amphibole from the NW, west, south and east cliffs. Other Montchal (*green*) and Mt. Sancy-type (*blue*) lava flows are shown for the purpose of comparison (after Brousse 1961; Bourdier 1980; Boumehdi 1988)

slopes are covered by a mixture of deciduous and coniferous trees that limit erosion. The region is characterized by an oceanic-mountain climate (Stebich et al. 2005). A mean annual temperature of 6.5 °C (between 1946 and 1974) was observed at Besse-en-Chandesse, the closest (4 km) meteorological station to the lake, located at an elevation of 1050 m asl. The annual thermal amplitude ranges between −5 and 20 °C (Stebich et al. 2005). Annual precipitation in the catchment averages between 1600 and 1700 mm. The climate diagram from this station indicates precipitation maxima in May and also between November and January. The lake surface usually freezes during the winter months while daily frost and thaw conditions may prevail between November and March (≥100 days/year in Besse's weather station located 150 m lower in elevation).

9.2.1 Geological Context Including Tectonic and Volcanic Features

Auvergne maars are typical landforms in the Chaîne des Puys (e.g. Beaunit, Gour de Tazenat), on the Mont-Dore stratovolcano (e.g. Chauvet) and in the Cézalier massif (e.g. Godivelle d'en haut). Pavin maar is the youngest volcano in continental France, which stands among a group of four volcanoes which erupted within a period of five centuries (Juvigné 1992a,b; Juvigné & Miallier, Chap. 9, in this volume). In chronological order (Camus et al. 1973), these are: Montcineyre strombolian cone 4 km south, Estivadoux maar 1 km southeast and Montchal strombolian cone adjacent to the Pavin crater to the south (Fig. 9.1). The regional map based on the IGN DEM (10 m pixel) shows the geologic context of the Pavin maar on the western flank of the Sancy massif, which is the youngest edifice of the Monts-Dore stratovolcano (Bourdier 1980; Lavina 1985). The maar cut away the high (210 m) north flank of the Montchal cone and its lava flows to the ENE (Figs. 9.1, 9.2, and 9.3). Montchal lava flows cut by the maar are older than the strombolian scoria-fall from the Montchal cone, which directly underlies (without any soil) the 6730 ± 130 year Pavin maar deposits. Porphyritic, trachybasaltic lava flows of Montchal, which were cut by the maar, surround the lake except on the NNE rim slope. There, the leucite-bearing tephritic lava flow that makes the fractured cliff shares mineralogical and geochemical characteristics with Mont-Dore Sancy lava flows as shown by the TAS diagram (Fig. 9.2).

The group of four volcanoes provides no evidence for a north-south graben. Lavina (1985) locates the Pavin-Montchal group at the southern end of a N105-125°E dyke group linked to the Sancy stratovolcano. Instead, the Pavin maar together with the Montchal and Montcineyre cones are roughly aligned N160° although no fault is observed at

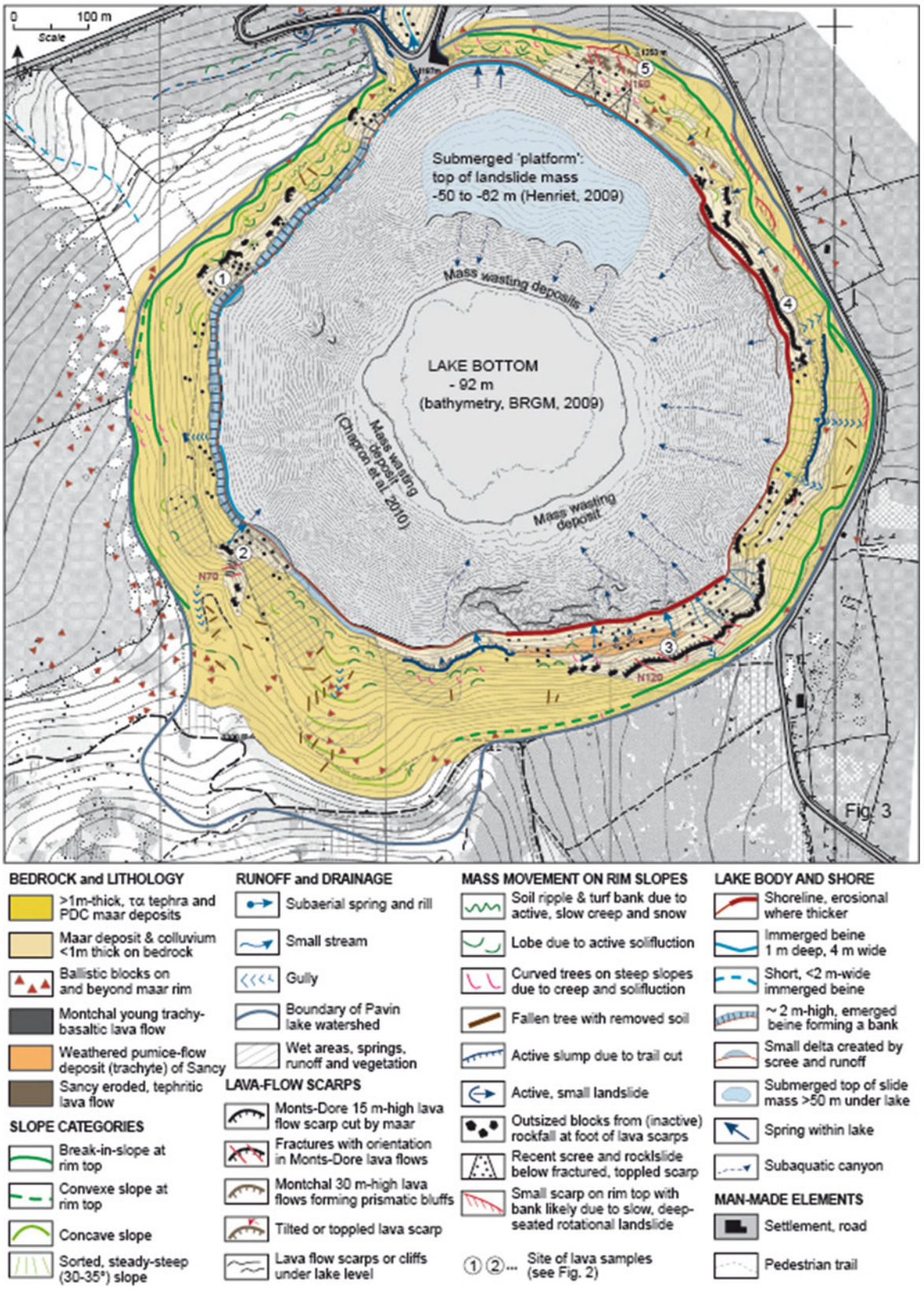

Fig. 9.3 Geologic and geomorphological map of the maar rim slopes with emphasis on slope landforms and inferred processes

ground surface. Fig. 9.1 portrays four groups of lineaments at the intersection of which the four volcanoes are located: (1) N10°E fractures appear west of Pavin (e.g. the Escarot mofette 3 km west of the lake extends 0.4 km N-S) and SSE of Montchal (Fig. 9.1), (2) N70°E lineaments guide large valleys in the region, (3) N110°E fractures which may offset N10° lineaments, and (4) N160°E fractures. These lineaments likely reflect deeper faults in the basement and the Pleistocene Sancy volcano.

The polygonal shape of the Pavin maar displays six sides, the most rectilinear of them (N10-20, N70, N110) paralleling lineaments shown in the tectonic sketch of Fig. 9.1. After almost 6700 years of existence, the non-circular shape of the maar rims suggests that the post-eruption slope erosion has been relatively slow under temperate climate conditions as vegetation probably covered the slopes soon after the eruption ended (e.g. Schwab et al. 2009). Another reason for the irregular rim is that the deep, funnel-shaped crater nested in lava rock together with resistant lava cliffs around the lake have preserved a large amount of the original maar form except the north flank of Montchal cone. Tops of maar rims still show a strong asymmetry (gentle outer slope versus steep inner slope) around three quarters of the maar except the wide, gently dipping and concave, north Montchal's flank over which maar tephra and cone scoriae have been redistributed since the maar eruption. The asymmetry of the crater inside the maar lake, as inferred from the bathymetry (*in* BRGM 2009), is due to the quasi vertical SE and east slopes cut in thick lava piles, which contrast with the subaquatic plateau submerged in the NNE part of the lake (Fig. 9.3).

9.3 Materials and Methods

Three categories of field and laboratory methods have been undertaken to map the maar and analyze its slope stability: geologic and geomorphologic mapping, very high resolution DEMs, and analysis of geomorphic parameters.

9.3.1 Geologic and Geomorphologic Mapping

Mapping of the maar rims has been conducted with students over the past 4 years in order to delineate surficial deposits and highlight landforms and processes that may indicate slope instability around the lake. Analysis of DEMs and delineating from aerial photographs taken by IGN in 1948, 1956 and 1962 were carried out with a stereoscope and completed by field observations. Deposits have been studied in the field and lava and tephra samples (thin sections, geochemistry and grain size distribution) were analyzed in the LMV laboratory (Boivin et al. 2012; Fig. 9.2). We had access to the old geologic map of Brioude (1964, no.175, scale 1:80,000) and the unpublished sketch map of Besse (after the name of the main town 3 km ENE of Lake Pavin) carried out by P. Lavina (BRGM Puy-de-Dôme).

The rim slopes map (Fig. 9.3) was drawn on a 1/10,000 scale topographic map with 10 m contours (Camus et al. 1993) outside the lake, to which a more precise, 1 m-contour bathymetry derived from a DEM was added (MESURIS Bathymetrie in: BRGM 2009). Two maps of the Gelat and Couze Pavin River valley were drawn on a 50 cm-pixel surface DSM (i.e. without filtering vegetation above soil), which represents a new basis for mapping landforms with unprecedented detail and allowing for a better interpretation of slope and valley processes. Thus, Figs. 9.4 and 9.5 display the bedrock, surficial deposits and mass movements along the Gelat – Couze Pavin valley adjacent to the north maar rim. We have focused on lithology, deposit types and landforms indicating mass wasting and mass movements on slopes at all scales.

9.3.2 Very High Resolution DEM Acquisition and Calibration

Over the past 10 years, Unmanned Aerial Vehicles (UAVs) have become relevant tools for high resolution Digital Elevation Model computation using stereophotogrammetry methods. A survey of the Plaine du Gelat area adjacent to the north maar rim was carried out in April 2015 to acquire a set of low-altitude photographs that can be used to compute high-spatial resolution DEMs. A fixed-wing drone (Lehmann Aviation LA300) was operated by Technivue society and equipped with a 12 Mpx Canon PowerShot S110 camera (focal length: 5.2 mm). The plane flew at about 200 m in elevation above ground using preprogrammed GPS positioning. A simple constructed two dimensional stabilization plant is designed to keep the image sensor's optical axis directed at vertical. Due to the limited battery capacity the grid based flight plan had to be subdivided into eight flights, allowing us to acquire a complete set of 2608 images, with a total coverage area of 4.17 km^2. As many as 908 images were selected to ensure an image overlap of about 80 % and side overlap of 30 % over the entire study area with a mean ground resolution of 0.068 m per pixel.

The photogrammetric workflow has been carried out using Agisoft PhotoScan software. Before the photogrammetric survey, 52 targets (50 cm-wide white squares) were installed in the field. Targets coordinates were measured using two Differential GPS (DGNSS) receivers (one being a fixed base) with a positioning accuracy of c. 2 cm. The entire set of targets was defined as Ground Control Points GCPs and manually positioned on the images. The resid-

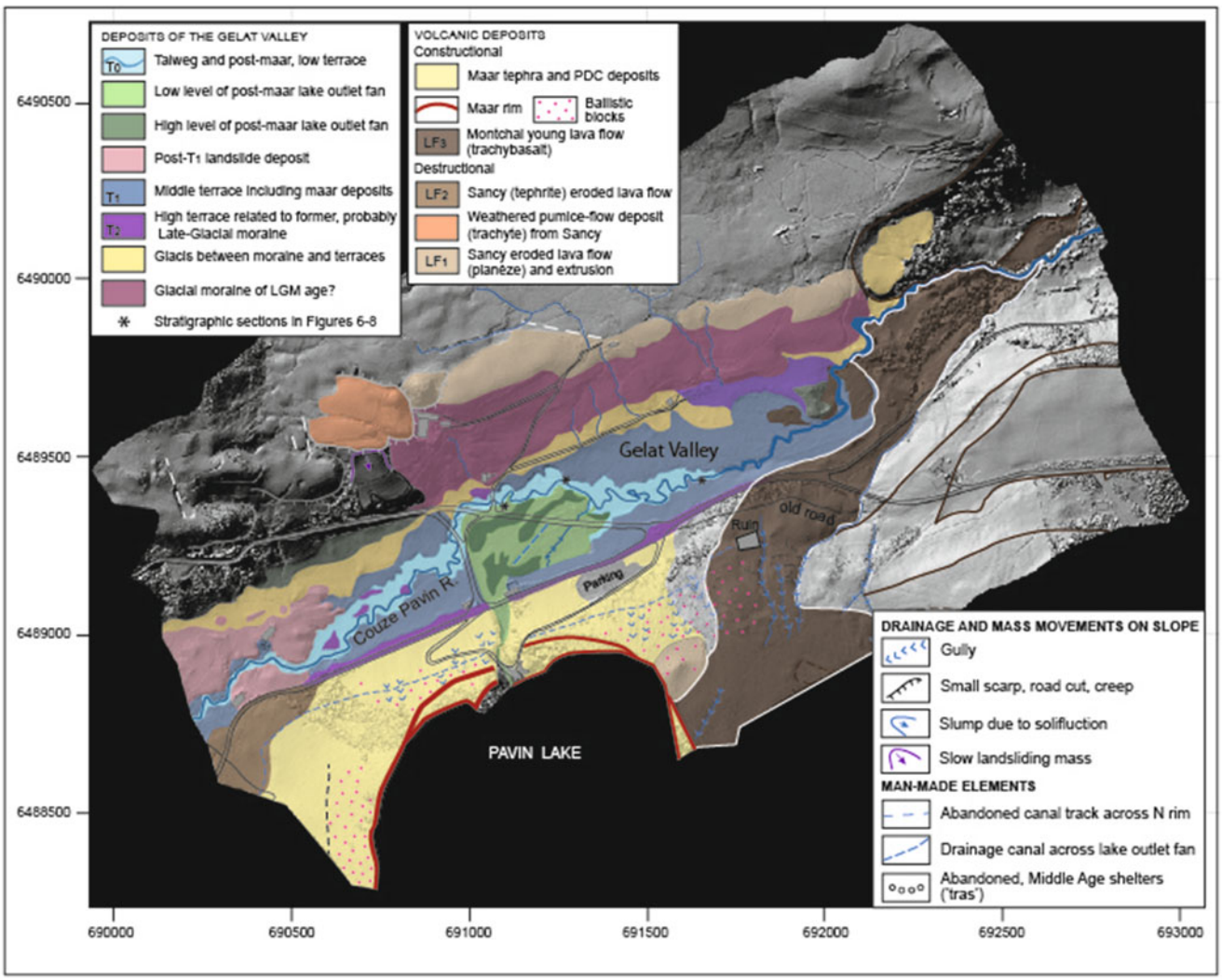

Fig. 9.4 Geologic map draped on very high resolution DSM (here cropped at 50 cm) showing a stratigraphic record of landforms in the Plaine du Gelat, middle course of Couze Pavin valley

ual difference between the models and the GCPs's coordinates was estimated by Photoscan to be more precise than 4 cm. The next step was the automatic matching of tie points using a feature based approach. The resulting tie point coordinates ($3.3 \cdot 10^6$ points) were used as observations in a robust bundle adjustment. The final processing step was the densification of the scattered 3D point cloud of tie points by a dense matching algorithm of the automated workflow in Photoscan. The resulting dense point cloud (density of 13.4 points per m^2) was used to derive the high resolution DEM, generated in the RGF93/Lambert93 projection (NGF IGN69 elevation), and the associated orthophoto of the entire scene. This drone-based multiview photogrammetry acquisition allowed us to compute a 25 cm-spatial resolution DSM (Digital Surface Model, including vegetation cover) with planimetric and altimetric accuracy of c. 5 cm.

9.3.3 Analysis of Geomorphic Parameters of the Maar and Lake

The Pavin maar belongs to the first category of Seib et al.'s (2013) geomorphological classification on the basis of five parameters (Table 9.1): rim diameter, rim height, rim height/diameter ratio, excavation depth and bedding dip (Vespermann and Schmincke 2000). Other parameters are tephra ring, angle of the inner rim slope, angle of the outer rim slope, diatreme depth and depth coefficient (e.g. Büchel et al. 1993).

Pavin maar large diameter (900 m) lies in the average values for maar crater diameters (0.7–0.8 km) albeit their entire range varies widely between 0.2 and 3 km. Pavin maar is wide to the point that the mean height / rim diameter ratio of 0.15 defines a high-relief depression at the upper end of the 0.13–0.05 range for usual maars. If we take into account the

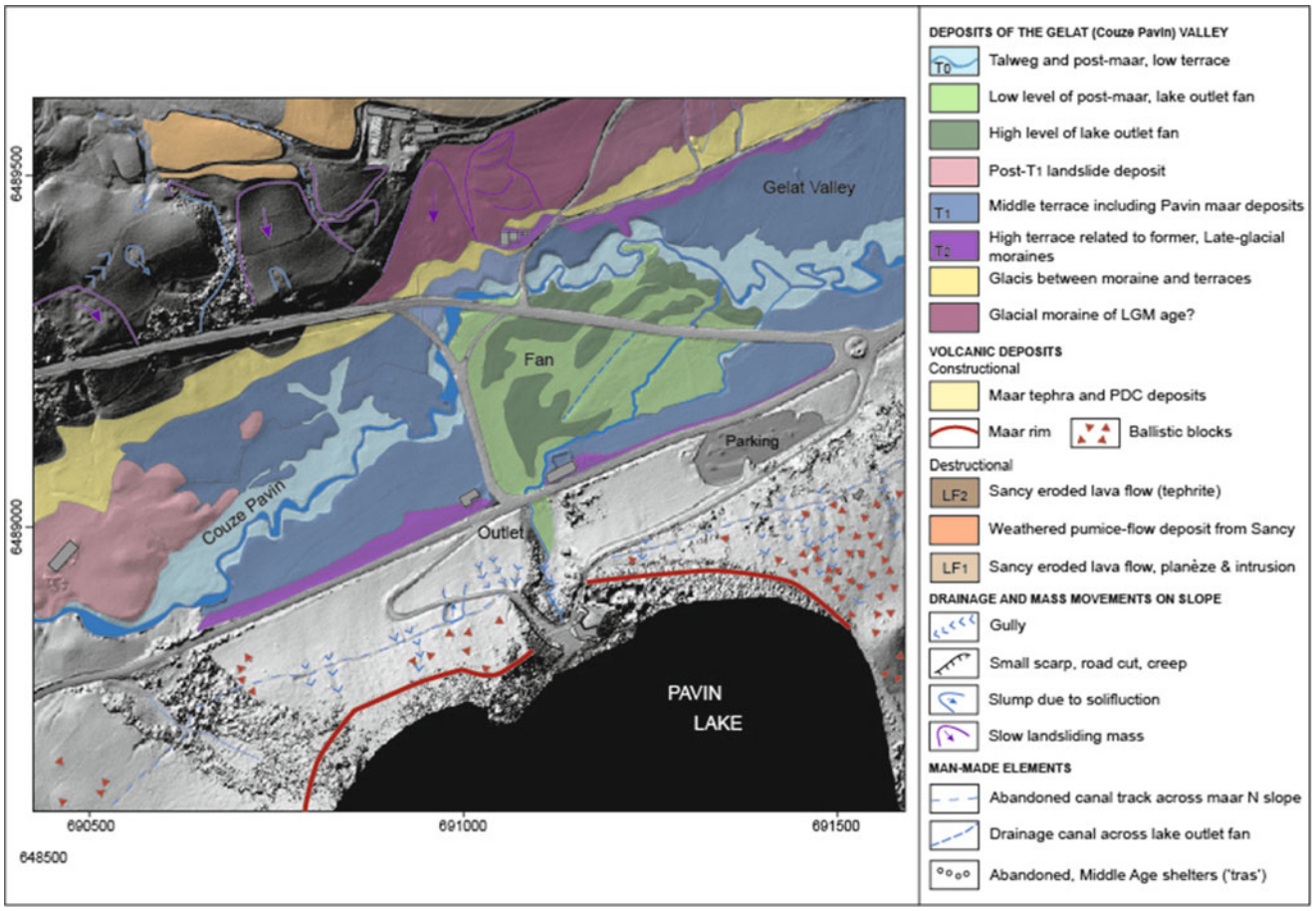

Fig. 9.5 Close-up geologic map draped on very high resolution DSM showing the alluvial fan created by the lake outlet in the alluvial terrace setting of the middle course of the Gelat valley

Table 9.1 Geometric and morphometric characteristics of the maar and comparison with average parameters of maars worldwide

Morphometric parameters	Rim diame-ter (km)	Mean/maximum rim height (m)	Rim height/diam. ratio	Excavation depth (m)	Mean/Max bedding dip (°)
Pavin maar	0.9	130/145	0.15	average 140	inner 30–45
		(56 above lake)		max 290	outer 10–25
Pavin	0.8	Na	0.05	92 max 102	deposits >30
Meromictic lake				incl. bottom turbidites	in lake
Min/Max size	0.2–3; aver. 0.75	Average 50	0.05–0.13	50–100	5–20

92 m crater depth under the lake surface and the highest rim elevation above lake (210 m to the SE), the latter ratio increases to 0.33. This contributes to the original and unusual depth coefficient of 0.18 accounting for the funnel-shaped 92 m crater depth (i.e. average maximum depth 145 m/√surface area (0.64 km^2). This relatively high depth coefficient together with the steep rim elevation facing prevailing winds from the WNW explains the limited wind and wave action inside the maar. This in turn favors the meromictic characteristic of the Pavin lake. The high relief of Pavin maar rims is enhanced if we account for the strong asymmetry between the short (≤0.1 km) inner slopes (30–45° on average, with vertical cliffs on the east and south flanks) and the wide (≥0.70 km), gently dipping outer slopes (<20° to the west). These become flattish eastward where the maar ring abuts low relief, young Montchal lava flows (Fig. 9.1). As a result, the shape of the maar Pavin is closer to a high and large bowl than the low-relief maar depressions in the Chaîne des Puys and Cézalier (e.g. Beaunit, La Godivelle d'en Haut). Further north-south asymmetry stems from the contrast between the highest (210 m) rim to the south, which coincides with the Montchal cone flank, and the low-relief

NNE rim <60 m above the lake level, with a notch (70 m wide) open in the rim towards the north.

Given the relatively young age of the maar (c. 6700 years) and the moderate geomorphic processes acting under a temperate mountain climate, the original shape of the subaerial depression has not degraded much over time; hence any post-erosion maar basin enlargement (Jordan et al. 2013) and shift of the geometrical parameter ratios can be neglected. In contrast, geophysical investigations under the lake have shown that the crater floor and rim have considerably changed with a flat central bottom covered by 5 m-thick turbidites, a submerged plateau with eroded edges and sectors between the bottom and the walls that are mantled by thick debris fans (Chapron et al. 2010a, b; 2012). The main processes having formed the shoreline shortly after maar eruptions are collapse events followed by the propagation and interfingering of debris fans. The largest debris fan in the lake is on the south but a submerged platform on the NE side of the lake is the top of a collapsed mass (Henriet 2009). If we consider the subaerial maar, the stage of erosion compared to other maars worldwide can be ranked two out of five after Büchel (1993) and one out of three after Németh (2001). If the maar-crater lake system is considered, the stage of erosion after c. 6700 years of existence does not fit the "filled stage" of Büchel (1993) or the "moderately eroded" stage of Németh (2001).

9.4 Geologic and Geomorphologic Mapping to Determine Slope Instability

9.4.1 The Maar Rim and Slopes

Figure 9.3 displays geologic and geomorphologic mapping of the rim slopes: bedrock and lithology, slope categories, runoff and drainage, lava flow scarps, mass movements on rim slopes, lake shore and man-made elements. Bedrock is shown only where maar deposit is less than 1 m thick. Bedrock lithology includes 'old' lava flows of Monts-Dore-Sancy, limited outcrops of weathered pumice-rich deposit from Sancy volcano on the south edge, and recent Montchal lava flows forming >30 m-thick cliffs cut by the maar on the eastern side.

The 15–30 m thickness of the rim sequence (BRGM 2009) is an average value for maars usually <50 m thick. Maar deposits covering the inner slopes at Pavin are massive and much less well bedded than the outer slope deposits 0.75 km ESE away from the maar (Boivin et al. 2012). Deposit is typically coarse sand and gravel, pumice- and clast-rich, trachyandesitic tephra 1- to 5-m thick on the steep inner slopes of the maar rims. The maar deposits are coarser than the average fine grained deposits that dip gently to less than a few degrees outward. Maar deposits encompass fine grained, bedded surge deposits, pumice-fall layers attributed to a sub-Plinian episode (Boivin et al. 2012) and massive pyroclastic-flow deposits totaling 2–5 m on the outer slopes of the rim. Accidental clasts are less abundant at Pavin than common maar deposits in which they may reach up to 90 % by volume. Maximal diameter of country rock fragments may exceed 2 m, which is not at odds with the 3 m maximal size of maar ejecta elsewhere. Strewn on the rim and outer slopes, ballistic blocks (commonly 1 m^3 and up to 4 m^3), now observed towards the west and WSW and towards the E and NE, suggest two prevailing angles for the ejecta dispersal (Fig. 9.5). Violent ballistic explosions expelled blocks exceeding 2 m across to a distance of 700 m while ballistics 1 m across reached 1.2 km from the crater (see Lorenz 2007, for a comparison of size/travel distance of maar ballistics).

Slope categories are based on slope aspect (exposure, angle) and the shape of the top rim slope. We emphasize the persisting break-in-slope at the top of the rim around three quarters of the maar circumference. Some maar rim slopes remain vertical as lava cliffs crop out on the eastern and southeast edges. Other maar rims on the NW, W, E and NE edges evolved from cliffs to short, rectilinear, sorted slopes close to angle of rest (31–35°) covered by only thin and sorted tephra or colluvium. Lava flow scarps drawn on the map (Figs. 9.3 and 9.6) include three cliff segments showing open fractures and toppling over with debris feeding screes below. Lava flows cut by the maar include: the 'older' Mont-Dore (Sancy) cliffs of basalt higher up on the maar rims and the 'younger' Montchal, trachybasalt lava flows which form 20–30 m high cliffs armoring the east rim. The thick Montchal lava flows were channeled in a valley cut perpendicularly by the eastern maar rim. One channeled lava flow has blocked the Gelat plain in the Couze Pavin Valley to the NE (Fig. 9.4) and continues beyond the town of Besse at a distance of 14 km down valley (Bourdier 1980; Boivin et al., 2009, pp. 118–119).

Runoff and drainage are fed by springs above and below the lake level. Springs are more abundant on the south and SE rims of the maar at the base of the Montchal cone as permeable boundaries exist between lava flows and the underlying, clay-rich, weathered pumice deposit of Sancy. Permanent springs and rills on the north Montchal flank supply water that favors runoff and slumps in the sector. Mass movements are observed on all rim slopes but prevail on steep slopes to the north, NE, NW and SE. We distinguish three types of mass movements based on size and processes (Figs. 9.3, 9.4, 9.5, 9.6 and Table 9.2).

1. Small (tens of m^2) forms such as soil ripples, turf bank terracettes are due to creep and solifluction. Slow slope processes are also indicated by curved trees and many fallen trees that remove soil and colluvium. Wet areas around springs with hygrophilous vegetation (Fig. 9.3) and a 3–5

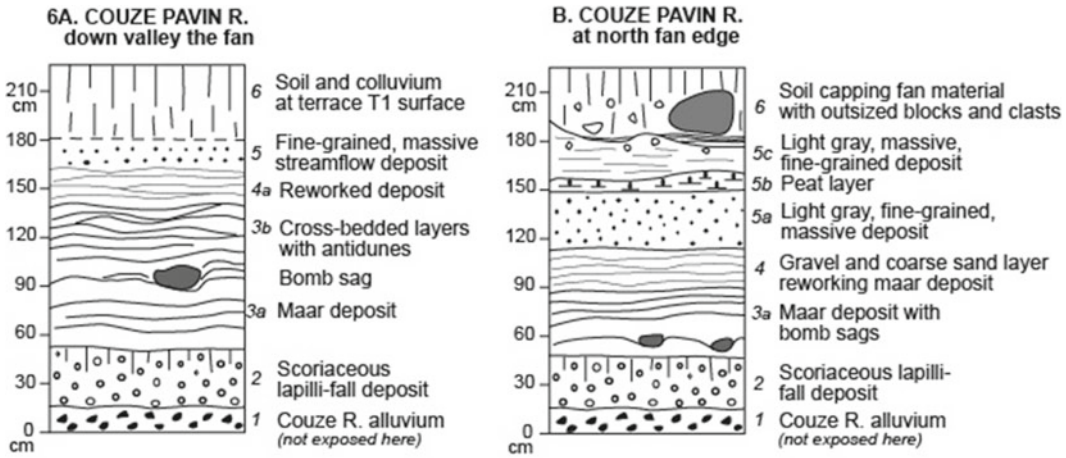

Fig. 9.6 Two stratigraphic sections located along the Couze River in the Gelat Valley north of the Pavin maar. A. Deposits observed in the terrace T_1 section on the Couze River south bank about 0.25 km downstream of the lake outlet fan. B. Deposits observed in the Couze River north and south banks at the northern end of the fan of the lake outlet

Table 9.2 Parameters used to assess and delineate hazard-prone areas around the lake Pavin and on the maar rims (including previous data from subaquatic investigations led by Chapron et al. 2010a, b)

Geomorphic areas	Slope categories	Landforms		Mass movement	Criteria for mass movements and slope evolution
		Erosional	Depositional		
Maar rim slopes	Break in slope at top, steady, rectilinear below	Cliffs	Tephra	Landslide	Top scars and banks, open fractures, failure plane
		Steep slopes	None	Rock fall rockslide	Chaos / scree
	Convex or multi convex-concave		Tephra cover	Solifluction	Concave scar and convex lobe, curved trees, soil deformation
	Irregular, undulated		Colluvium, soil	Creep	Small turf banks, soil ripples (snow cover)
	Concave, incised		Alternate layers	Gullying	Drainage: sources, streams, heavy rainfall
Lake shore	Above line	Emerged Subaerial	Immerged	Lake oscillation?	Riverine bank >2 m high above N,W&SW shoreline
	Under line	beine?	beine	Artificial level rise	Coarse deposit >1 m deep below shoreline
Lake outlet and adjacent Gelat Valley		Outlet fan			Two levels of deposits
					Canal drainage
		Terraces T_1-T_3			Inset channel deposits

month-long snow cover favor solifluction as do persisting firn on north aspect slopes.

2. Relatively small landforms tens to hundreds of m^2 in size are rock fall blocks below small or thin lava scarp (SW, NW) or recent scree slopes below fractured lava flow scarps to the NE. Rock fall is not a continuous process as witnessed to by moss and lichen covering boulders. Stacked, outsized blocks (up to 10 m across) form chaos below small fractured cliffs, e.g., on the NW and SW rims and the longest scarp of Mont Dore-Sancy lava flow on the SSE rim. This cliff <200 m long and 10–20 m thick shows open fractures and many blocks below (Fig. 9.6). Rock fall is a discontinuous process as several blocks meter sized, not covered by moss or lichen, are sliding on the steep and wet slope cut on clay-rich material below the cliff foot. These lava flows show pervasive fractures oriented N160 on the NNE rim, N120 on the south rim and N70 on the SW rim. They parallel regional lineaments portrayed in the tectonic sketch of Fig. 9.1. Recent scree may result partly from cliff rock shuttering due to frost/thaw effects that produced debris accentuating scree and rock falls (NE and SSE slopes) during the Little Ice Age. Cold spells occurred during the sixteenth and seventeenth centuries on the basis of pollen and diatom fluctuations recorded from cores collected in the lake sediment (Stebich et al. (2005), Schettler et al. (2007) and Schwab et al. (2009). Yet, scattered blocks still fall from the fractured cliff as they

remain lichen-free and blocked by young trees at the foot of the lava scarps.

3. The third landforms are more subtle such as small (2–4 m high) scarps and adjacent banks near the rim top on the NE and east side of the maar (Fig. 9.3). On the NNE rim top, a scarp overhanging the adjacent bank associated with a shallow gully forming a scar, together with curved and fallen trees around the scar, suggest a (slow?) process of deep-seated rotational landslide. This coincides with the top of a landslide mass (attributed to the maar eruption based on the ^{14}C age of the base of the overlying sediment) forming a platform at −42 m in the lake at the base of the NNE rim slope. Failure plane may correspond to the contact between the maar tephra deposit and bedrock or along impermeable layers within the tephra deposit. Other scarps and banks on the east rim top show no scar or curved trees.

9.4.2 The Lake and Riverine Maar Rim Contact

The lake occupies 0,445 km^2 in area and hosts a water volume of about 24.1 million m^3. Pavin is known to be the only meromictic lake in Auvergne, which consists of two superimposed and geochemically different water bodies, termed a mixolimnion above a monimolimnion (Jézéquel et al. 2008). This characteristic is related to the unusual lake depth coefficient as a result of the funnel-shaped, deep crater inside a relatively high-relief maar ring.

The riverine lake contact can be divided in two areas, one immerged and another subaerial, separated by a bank a few meters high. Half of the lake shoreline is erosional (near lava cliffs) while the other half is depositional (concave slopes covered by screes) (Fig. 9.3). The erosional shore, which prevails on the east and south edges of the funnel-shaped crater lake, is characterized by a narrow shoreline above deep water without a *beine* (subaquatic terrace). This is the usual case of lakes in erosional context where the riparian bank directly overhangs a submerged beine at the water contact (Provencher and Dubois 2008; Touchard 2000). Lake Pavin shows no high water level due to heavy rain inflow so the present-day shoreline corresponds to the stable high water lake despite limited seasonal fluctuations. Accumulation shoreline includes a 1 m-deep, immerged beine along the western and NE edges, which can reach 4 m wide above deep water steep slopes. Locally (SW, NW and at the foot of the Montchal lava bluffs to the east), a narrow beine has been formed by screes or rock falls from adjacent cliffs (Fig. 9.3). On the western lake edge the beine is slightly larger due to runoff, tephra redistribution and scree or rock fall. Screes and runoff have formed small deltas in the NW and SW corners of the lake. The erosional and depositional pattern of the lake shore is also a result of wave action, which is more important on the eastern edge than the western side. Primary wind direction is from west-northwest. The lower north, NNW and NNE crater rims provide less shelter against the wind and the longest lake diameter from NNW to SSE with the highest fetch is oriented in a SE direction. However, wind action on waves is limited by the high maar rims and the funnel shape of the maar-lake system.

The immerged beine observed near the west and north shoreline is largely due to recent anthropogenic impact. The level of the lake was artificially raised in 1859 when works (allowing noble fish introduction) heightened the lava threshold and covered the outlet. Today a large platform exists at the northern entrance of the maar for touristic and access purpose where the maar rim was the lowest originally.

9.4.3 Possible Links Between Subaerial Slopes and Subaquatic Landforms

When slope angles in Lake Pavin are above 31°, they are free of any sediment and characterized by the development of numerous steep canyons clearly visible on *multibeam bathymetric* data (Figs. 23.4, 23.7 and 23.10; Fig. 9.3). As sub-bottom profiles along steep slopes only illustrate the morphology of the acoustic substratum, Chapron et al. (2010a, 5e; Figs. 23.5a, 5d) claimed that these canyons draining the steep slopes of Lake Pavin crater are still active path for sporadically bypassing sediment towards the deep central basin. In such a context it is highly possible that sediment from subaquatic littoral environments, lake shores and subaerial slopes from the crater ring draining into the lake can be exported directly to the deep central basin (Fig. 23.10). Abundant sources near the lava cliff and streams cutting the south and SE subaerial rim slopes probably continue in the lake as gullies and 'subaquatic canyons' described across the south flank of the crater (Fig. 9.3; Chapron et al. 2010a,b).

Mapping suggests probable relations between topographic anomalies reflecting mass movements on the NE rim slope with the submerged landslide mass in the NE lake sector (Figs. 9.3 and 9.6). Chapron et al. (2010a) related the slump deposit ^{14}C dated and calibrated between 580 and 640 AD (PAV08 site) above the subaquatic platform and the most recent scree slopes on the NE maar rim. The fractured 'old lava' cliffs on the north flank of Montchal are only the subaerial part of a pile of immerged lava flows that are drawn along the south rim edge (Fig. 9.3). Locally, >45° slopes at the eastern and southern edges of Lake Pavin coincide with outcropping, unstable lava cliffs within the inner slopes of the crater ring (Figs. 9.3 and 9.6; Chapron et al. 2010a). Blocks along the shoreline and reported on the steep slopes near these lava cliffs highlight the occurrence of relatively small sized but recurrent rock falls.

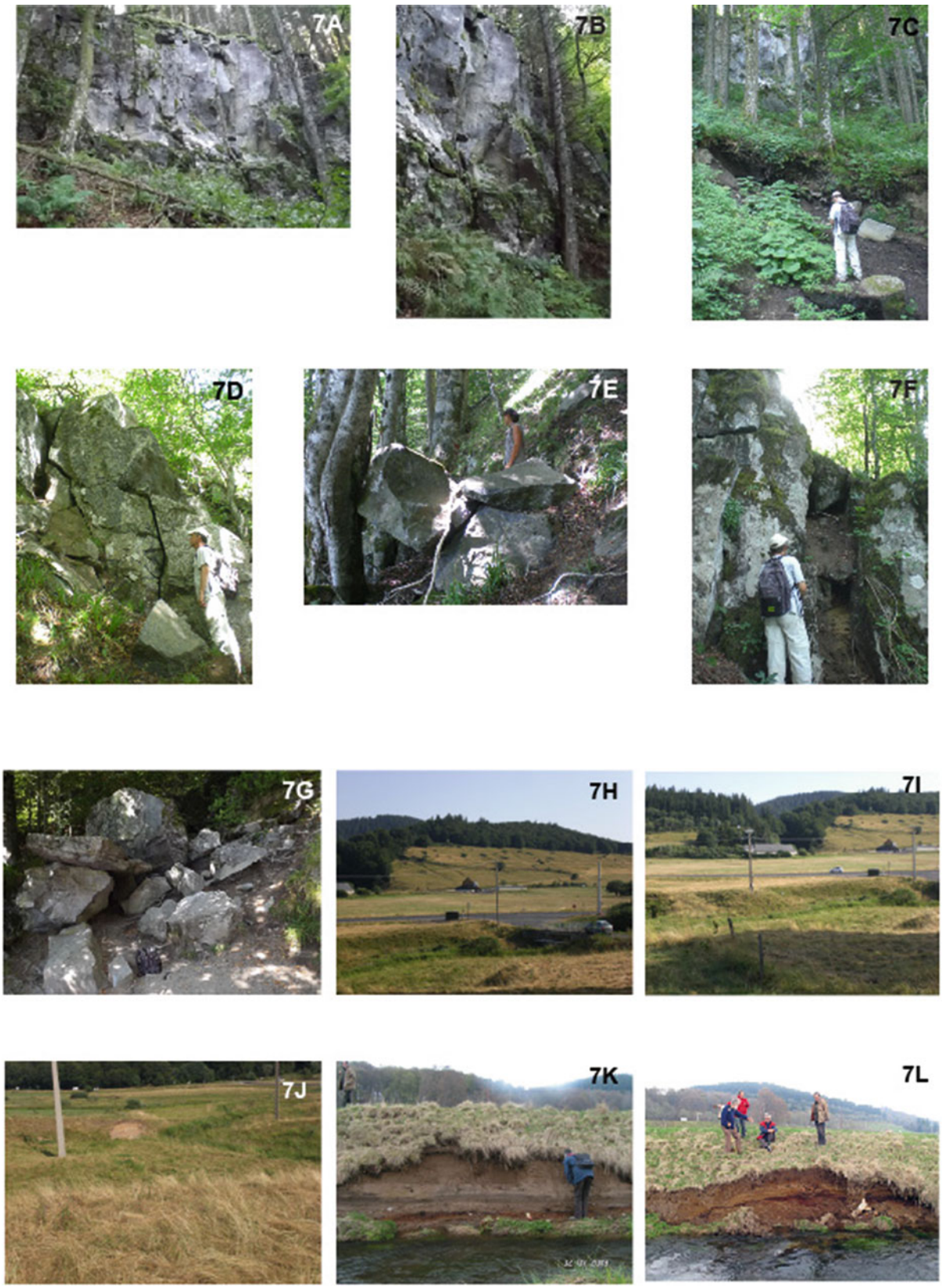

Fig. 9.7 Pictures (©J.-C. Thouret and D. Miallier) showing relevant landforms, deposits and mass movements around the maar lake and in the Gelat Valley. (**a**) Cliff of trachybasalt lava flow below the Montchal scoria cone on the SSE edge of the maar. (**b**) Note fractures and topple across the 12 m-thick, trachybasaltic Montchal lava flow scarp. (**c**) Scar of slip, spring and runoff on weathered, Sancy pumice-rich pyroclastic deposits overlain by the Montchal lava flow. (**d**) Fractured cliff of Mt. Sancy tephrite lava flow, NNE slope of the maar. (**e**) Fallen blocks retained by young trees below the previous cliff are not covered by moss or lichen. (**f**) Open fracture in the Montchal trachybasalt lava flow, SW slope of the maar. (**g**) Chaos of outsized boulders below an eroded cliff of Montchal lava flow at the foot of the NW rim cliff.

9.4.4 The Lake Outlet and Fan

We have mapped the landforms of the Couze Pavin Valley adjacent to the maar, termed Plaine du Gelat, including a geologic and geomorphologic map draped over a very high-resolution DEM (see 9.3.2) together with a close-up map of fan deposits associated to the lake outlet in the middle reach of the Plaine du Gelat.

The first map (Fig. 9.4) shows the alluvial and glacial deposits of the Gelat plain, the volcanic deposits of the Monts Dore east flank, the Montchal lava flows and Pavin maar deposits, and finally mass movements on slopes. Pre-Pavin maar deposits are represented by Monts Dore (Sancy) basalt lava flows and trachytic pumice-flow deposits from the Sancy massif (associated to the Sancy caldera by Lavina 1985). Glacial moraines cover the flanks of the valley particularly the north one. On the south flank, the lava flow from Montchal, which was channeled in a valley and flowed towards the Couze valley, dammed the Plaine du Gelat. The north outer rim of the maar shows solifluction lobes and shallow gullies cutting down the thick maar deposit. Most gullies seem inactive or subdued. A sub-horizontal, subdued track on the slope marks out an abandoned, historic drainage canal that extends from the NW slope and crosses the outlet ravine towards the east along the south slope of the Gelat valley (Fig. 9.4).

Figure 9.5 is a close-up map of the central part of the Gelat Valley just north of the maar lake in which the lake outlet formed a fan. The Pavin lake small outlet (mean discharge 50 l/s) feeds a stream draining a ravine open to the north, 50 m wide down valley and 40 m deep below the lava scarp threshold that dammed the lake (visible in the historic Lecoq painting of 1867). Adjacent to the outlet tunnel, an iron-bearing source has been shown to result from outward drainage of the bottom lake (monimolimnion) (Jézéquel et al. 2008). The stream has formed an alluvial fan starting at the foot of the rim slope of the maar at 1175 m asl. The subdued fan that extends 250 m towards the north and 300 m NE across the Gelat valley, pushed the Couze River against the north valley bank (Fig. 9.5). In turn the Couze River became meandering as the fan blocked the valley and lowered its topographic gradient to as little as 1.1 %. We distinguish two levels in the fan formation based on close inspection of the very high resolution DEM (Fig. 9.5). High level, subdued deposits have been left by successive ridge axes of alluvial deposits when the fan was formed by repeated outlet floods. Low level, flattish deposits of the fan between bar bumps have been abraded by floods and smoothed out by runoff. The present-day topography compared with aerial photographs of 1956 reveals that the fan surface has also been modified by drainage canals and smoothed out by cultivation techniques.

9.4.5 Deposits of the Gelat Valley and Lake Fan

The Gelat Valley bottom and banks contains four types of terraces as follows (Figs. 9.4, 9.5 and 9.6): (1) The lowest T_0 lies near the bottom of the river channel that meanders (slope <1.5 %) upstream of a rockbar. This rockbar corresponds to Mont-Dore lava flows overlain by the Montchal channeled lava flow. (2) The middle T_1 terrace in which the Couze Pavin River channel is cut down about 3 m, contains the maar deposits, which have been reworked by streamflow processes (Figs. 9.7 and 9.8). (3) Remnants of the middle T_2 terrace are observed on both sides of the valley about 4 m above the channel. This terrace can be linked to a valley bottom enclosed by moraines of Late or Full Glacial age or to alluvium released by former glaciers upstream of the valley. (4) Landslide deposits have covered the T_1 terrace, triggered by landslides the long and deep scar of which is visible on the north flank of the valley.

Figure 9.6 shows the stratigraphic succession of six deposits associated to the terraces of the Couze River and the fan formed by the lake outlet in the Gelat Valley. Deposits no.1–6 are illustrated in Figs. 9.7 and 9.8. On the south bank of the Couze Pavin River ~0.35 km down valley from the fan, the 3 m-thick T_1 terrace is 2.5 m lower than T_2 (Fig. 9.7j). Overlying the coarse, reddish, oxidized alluvium deposit 1 and the Montchal scoria-fall deposit 2, the 1-m thick, massive and fine-grained maar deposit no.3a is in turn overlain by a grey, cross bedded surge deposit 3b showing 2 m wavelength antidunes (Fig. 9.7k). Bomb sags have deformed the muddy, silt and sand-sized, stratified layers of the maar surge deposit 3a from left (SE) to right (NW) (Figs. 9.7l and 9.8a,b).

On the Couze River north bank section (Fig. 9.6a), the surge deposit 3b of the maar grades up in a massive, fine grained deposit (Figs. 9.7j, 9.8c, d). Lenticular, 50 cm-thick, sand and gravel layers filled the undulated, eroded top surface of the maar deposit pointing to a streamflow deposit 4a. (Fig. 9.8c, e). The layers grade up into stratified layers of sorted sand deposit 4b, which indicate that sand was

Fig. 9.7 (continued) (**h**) Gentle (<20 %) north outer slope of the maar showing undulated landforms due to solifluction and a network of inherited gullies. (**i**) View of the alluvial fan (note two *top* surfaces) at the mouth of the ravine formed by the lake outlet that has cut deeply down the north maar rim. (**j**) View of the T_1 terrace on the Gelat valley south side cut down c. 3 m by the Couze River channel, and fan surface in the background. T_2 terrace, 2.5 m higher than T_1, is visible in the background. (**k**) The T_1 deposits (geologist for scale) on the south bank of the Couze Pavin River ~0.35 km down valley from the lake outlet fan are described in Fig. 9.6a. (**k**) T_1 terrace shows the maar deposit 2 overlying the oxidized alluvium and Montchal scoria-fall deposit 1. The massive, fine-grained maar deposit is overlain by a *grey*, cross-bedded surge deposit showing 2 m wavelength antidunes. (**l**) The Pavin surge deposit 3a including bomb sags overlies the coarse, reddish Montchal scoria-fall deposit 2 mixed with alluvium

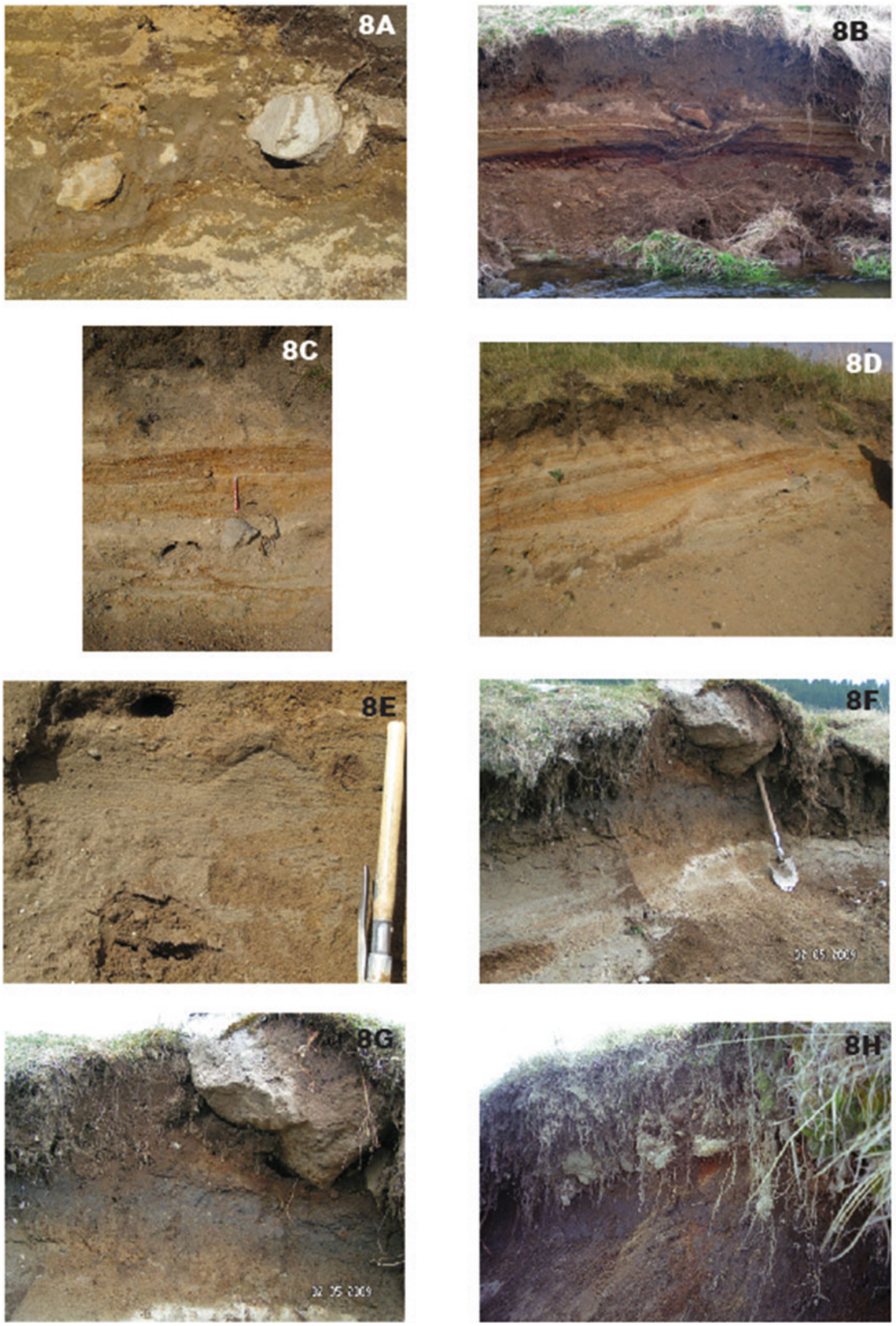

Fig. 9.8 Pictures (©P. Boivin, D. Miallier) showing the stratigraphic succession of six deposits associated to the terraces of the Couze River and the fan formed by the lake outlet in the Gelat Valley (see Figs. 9.6a, b). (**a**) Close up view of two bombs sags in the muddy, silt and sand sized maar deposit 3a. (**b**) Stratified, cross-bedded layers of maar surge deposit 3a impacted by bomb sags above the oxidized lapilli-fall deposit of Monchal. (**c** and **d**) Gravel and coarse sand layers 4a about 0.5 m thick fill shallow channel cut down in the undulated top of the maar

emplaced in a low energy alluvial channel. The uppermost, massive bed of coarse sand including small gravel suggests a flood deposit 4b associated to river overbank in a flat-lying alluvial plain (Fig. 9.8e). Although the section of the north bank of the Couze terrace T_1 is located near the northern toe of the fan, the sand and gravel, streamflow layers 4a show no evidence for catastrophic erosion above the contact with the maar deposit. Outside the fan and along the Couze River banks, 0.50–1 m-thick colluvium and soil (no. 5 in Fig. 9.6a) cap the T_1 terrace.

At the northern toe of the fan, the south bank section shows two additional deposits (Fig. 9.6b). First, a peat layer deposit 5 (dating in progress) overlies the sorted, sand layer 4b (Fig. 9.8e, f). The peat layer suggests that the flat, alluvial Gelat plain was impounded due to damming downstream. Brief impoundment is further suggested by the peat layer being intercalated between (a) a whitish, laminated, fine-grained deposit 5a beneath the peat layer and stratigraphically equivalent to the deposit 4b of Fig. 9.6a, and (b) a gray, massive and fine-grained deposit 5c above the peat layer, pointing to overbank deposit. Second, angular boulders and small clasts in thick, coarse fan material deposit 6 overlie the deposits 5a-c (Fig. 9.8g, h). The outsized blocks and angular clasts may have been emplaced by a combination of processes: (1) Glangeaud (1916) described scattered ballistic blocks strewn at the surface of the fan north of the maar. They no longer appear at the fan cultivated surface but the largest blocks may have been tossed aside by local farmers at the field boundary near the Couze Pavin channel; (2) clasts may have been transported from the maar north rim when the (pre-?)historical fan was formed by lake outlet floods, and; (3) some boulders may have been washed out by the Couze River floods from the moraines that mantle the valley slopes and from landslide deposits that covered the T_1 terrace upstream (Fig. 9.4).

9.5 Discussion

9.5.1 Observations, Criteria and Uncertainties on Lake and Slope Instability

We discuss relationships between slope processes and the evolution of the maar, potential links with subaquatic landforms described by Chapron et al. (2010a,b; 2012), and past climatic conditions. Slope erosion usually takes place right after the maar eruption and ceases when the tephra ring is stabilized by a cover of vegetation or becomes indurated diagenetically. Studies of young maars such as Ukinrek 1977 in Alaska (Pirrung et al. 2007) and young (1913) tuff ring in Vanuatu (Németh and Cronin 2007) have both pointed out that gullies and sheet erosion occurred shortly after the eruption and the following few weeks to months at most. The denudation of tephra proceeds at significantly lower rates compared with the retrogressive erosion of the inner crater walls. Height of crater rim decreased –whereas mean crater diameter increased as the horizontal central area of the crater floor is formed during first years of a maar. Re-sedimentation is due to collapse of nearly vertical parts of crater wall and undercutting of debris fans by waves. Water erosion lowers the tephra ring, widens the crater and deposits eroded material both inside the crater and also outside the tephra ring. As a result, the long term (at least tens of thousands of years), erosional enlargement of the maar leads to an unusually large basin with a relatively low surrounding rim (Németh et al. 2012; Jordan et al. 2013).

Evolution at Pavin consisted in redistribution of tephra mostly on the outer rim slopes which are much gentler than the inner slopes. Sheet runoff on outer slopes and some small gullies are apparently inactive today--except in cases of heavy rainstorm or intense forest clearing and cattle grazing during the Middle Age and the eighteenth–nineteenth century (see shelters locally termed 'tras' of that age in Figs. 9.4 and 9.5). Pavin maar inner slopes show limited tephra redeposition as the NW, NE and East sides cut cliffs or bedrock covered by thin soil and colluvium. On the SSE edge of the lake, runoff and rainwater streams, slumping and rock falls have removed and are slowly redistributing tephra on slopes. In contrast, maar tephra together with scoria material from Montchal was widely re-distributed on the north slope of the cone towards the lake.

9.5.2 Implications for Natural Hazards

Figure 9.8 displays six types of rim slopes according to degrees of instability. Instability has been determined based on a series of geomorphological criteria determined in Table 9.2. We also took into account the unpublished survey carried out by the regional BRGM office (BRGM 2009). Based on a set of parameters, we distinguish five types of unstable areas on inner slopes around the maar rim. The six categories are as follows:

Fig. 9.8 (continued) deposit on the north bank of Couze River. (**e**) Close up of the 50 cm-thick gravel and sand sized layers (deposit 5a) beneath the colluvium and soil six capping the T_1 terrace. (**f**) Angular blocks in the coarse fan deposit 6 overlie a light gray, massive and fine-grained (overbank?) deposit 5c and a peat layer 5b at the northern edge of the fan (Fig. 9.6b). (**g**) Close up of the peat layer 5b (dating in progress) interbedded between deposits 5a and 5c. (**h**) Large (50 cm) boulder and clasts at the base of the fan deposit 6. See text for possible processes that have emplaced the blocks

(1) Unstable, quasi vertical slopes on fractured cliffs with rock fall or steep landslide mass; (2) Potentially unstable, steep (31°) slopes on non-fractured cliffs, small mass movements in wet areas and/or gullying; (3) Relatively slow and surficial slope processes due to creep, solifluction and runoff; (4) geomorphological anomalies such as scarp-bank, scar suggesting top of deep-seated rotational landslide or collapsing mass; (5) Potentially unstable, subaquatic areas, and (6) rim areas with very little or surficial signs of erosion and mass movement. Figure 9.8 also suggests possible links between subaerial and subaquatic unstable slopes (based on published data for subaquatic landforms). Potentially unstable areas are the edge of the subaquatic plateau to the north and the pile of cliffs under the lake in front of the unstable cliff on the SE edge of the maar. The >30° slopes below the Montchal cliffs on the east side of the lake may be another potentially unstable area. Subaquatic plateaus, which are common in maar lakes (Chapron et al. 2012), represent the most probable potential sedimentation source area for mass wasting events along their sub-vertical edges. The authors reported a slump deposit 580–640 AD on site PAV08 on the platform not far from the most recent and wide scree slopes on the NNE rim. A large slide scar at 50 m water depth coinciding with the platform edge (Fig. 9.3) has been attributed to an event 1200–1300 AD. Chapron et al. (2010a,b) assigned these events to time periods when contrasted climatic conditions and lake level fluctuations occurred elsewhere in France, although strong evidence in Lake Pavin is lacking. Additional mass wasting deposits have also been reported on the SW and SE edges of the lake bottom (Fig. 9.5). Instability factors including the gas content of the lake sediments in the monolimnion have been pointed out by Chapron et al. (2010a, b)) & Meybeck (Chap. 3 in this volume). The occurrence of past limnic eruptions, however, has yet to be demonstrated (Fig. 9.9).

Has a higher, thus older, lake shore ever existed? The fact that a large (2–4 m) bank extends at least 2 m above the subaerial lake shore bank around the north, northwest and west edges, now used as a large trail, suggests the existence of a higher, older lake shore (emerged beine). We found no lake sand or silt layers as evidence for a lake shore on this bank, although the absence of lake sediment is not necessarily a criteria: this may be due to the limited wave action and lake level fluctuations. As the Pavin lake is not stirred by wind and its level does not fluctuate due to heavy rainfall today, it is difficult to find any evidence for lake sediment above the immerged beine and shore bank. However, pointing to a former high lake stage, Bruyant (1909) reported tracks of a previous weir of the lake. Bruyant mentioned a stair with a waterfall cut 4.84 m high above the 1909 lake level into the east slope of the present-day entrance. The platform now seen with a fence above the outlet 1 m above the lake level was erected in 1859 by Lecoq and Rico for fish breeding purpose. Bruyant (1909) also mentioned the existence of a canal whose intake was 0.21 m below the present platform and that provided water at least until about 250 years ago over 3.5 km east of Lake Pavin to the village of Olpilière 0.5 km south of Besse. We now observe the track of another canal several meters below the lake level on the north side of the maar rim running west to east (Figs. 9.4 and 9.5). Scars of slumps are located at the downstream side of the abandoned canal on the north rim slope now showing active solifluction landforms. We note that human induced erosion on the maar slopes (in particular during the 14–15th and nineteenth Centuries; Schwab et al. 2009) has been deduced from pollen studies, but historic impact has not triggered a large sediment flux comparable to that computed from other lake sediments in more populated Auvergne areas over the past 2000 years (Sarlième marsh: Macaire et al. 2010, and Aydat lake: Lavrieux et al. 2013).

Is there any evidence for lake overbank and outburst? On the one hand, the bank on the north and west side of the lake suggest a high, emerged beine while the perched weir 4.84 m high at the entrance points to a high lake standstill perhaps a few centuries ago. On the other hand, the deep and narrow ravine of the lake outlet shows no sign of catastrophic lake outburst. The boulders that pave its channel 0.2 km down valley probably slid on the slopes of the ravine from which runoff has washed them out of the rim deposit. In addition, no debris-flow deposit was found in the fan deposit created by the lake outlet except reworked maar deposits forming alluvial, gravel lenses towards the top of T_1 terrace. The platform has reportedly been slightly eroded (0.21 m?) since 1859 (Bruyant 1909) and Lecoq drawings (1867). The lava threshold is not going to collapse anytime soon but retrogressive erosion at the base of the outlet gorge will act in a long-term. Within the lake slumping on the edge of the subaquatic platform may occur and eventually destabilize the gas-rich turbidite cover on slopes and at the bottom of the lake, although hydrostatic pressure will prevent violent degassing. In addition, methane is present in the monimolimnion whereas its CO_2 content remains low (Camus 1993; Jézéquel et al. 2008).

Effects of tsunamis or lake seiches are beyond the scope of this chapter, but the reader is referred to Freundt et al.'s (2007) review of physical conditions for triggering and transferring waves in a lake. Seismic shaking, which would fluidize buried mass-wasting deposits in lake sediments, has been invoked by Chapron et al. (2012), but epicenters of reported earthquakes occurred far away and no sizable seismic activity has been recorded since instruments were deployed in Auvergne in the 1960s and around the lake by OPGC in 2009. More probable are oscillations in lake level such as those reported from Lake Albano, Colli Albano volcano, Italy, where overflows have repeatedly triggered lahars and caused damage down valley (Anzidei et al. 2008). Oscillations may be due to heavy rainfall storms and trigger lake waves

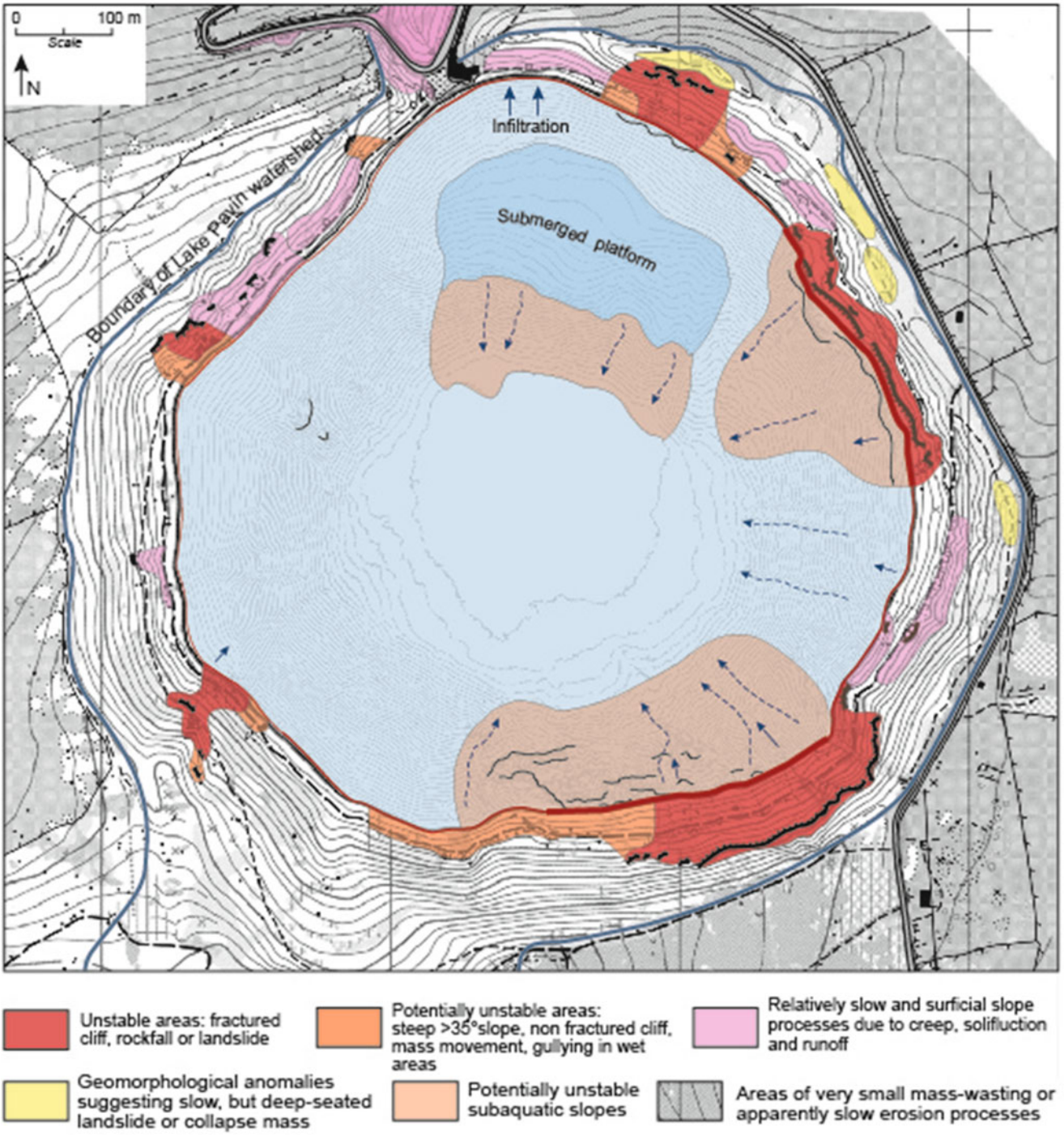

Fig. 9.9 Map of the Lake Pavin maar rim showing six categories of unstable areas: (1) Unstable slopes, (2) Potentially unstable slopes; (3) Relatively slow and small-sized slope processes, (4) Geomorphic anomalies suggesting slow but deep seated rotational landslide and/or collapse mass; (5) Potentially unstable subaquatic areas (Chapron et al 2010a, Henriet 2009); (6) Rims showing apparently very small or very slow slope processes

and seiche by resonance on lake edges. One of these exceptional storms and flooding events was reported in Auvergne around 580 AD (Vernet 2013), which may coincide with the slump of this age reported by Chapron et al. (2010a). Recurrent flooding events and the doubling of the background sedimentation rate since the early Middle Ages have been reported from the lake Aydat 27 km NE of Pavin (Lavrieux et al. 2012).

9.6 Conclusion

In contrast with postulated lake outburst catastrophic events, we found no evidence outside the lake for major lake breakouts or debris-flow deposit in the adjacent Gelat valley. However, multiple indicators for relatively slow and small sized, but numerous mass movements are observed on the steep inner slopes of the maar. Some sectors of the steepest rocky rims may pose a short-term hazard for people walking on the round-the-lake trail in particular at the foot of the south, SW and SE sectors of the maar. We also suggest that deep-seated rotational landslides may occur slowly on the NE rim, although a coupled *in situ* and laboratory geotechnical approach is needed to unravel whether this hazard is recurrent. The NE slope overhangs the subaquatic platform located on top of the syn-eruptive landmass that collapsed east of the entrance of the lake. In the absence of a large and/or near epicenter earthquake, however, it is not expected that a small (tens of m^3) to medium size (hundreds of m^3) cliff rockslide would trigger a wave in the lake that would overrun the lowest rim to the north. It is hoped that measures can be taken around the lake trail in the south and SE slopes and in two restricted areas to the SW (trail to Montchal) and NE (near the restaurant) in order to avoid the effects of potential rock falls. Drainage should be implemented below the lava cliff above the SE lake shore in order to avoid earthflows in case of exceptionally heavy rainfall. If the lake oscillations become sizeable in the near future, the drainage of the lake can be ensured by resizing the diameter of the outlet tunnel below the entrance platform.

Acknowledgments J.C. Thouret acknowledges all undergraduate students of the Department of Geology who have been mapping the maar surroundings under his supervision over the past 4 years. Thin sections and analysis of major elements have been carried out by C. Constantin, M. Benbakkar (LMV), and J. Marin (CRPG). Artwork has been achieved by L. Thouret. The content of this chapter has benefited from careful reviews and comments from our colleagues J.L. Bourdier, A. Gourgaud, E. Juvigné, D. Miallier, K. Nemeth, and C. Ollier.

References

Albéric P, Jézéquel D, Bergonzini L, Chapron E, Viollier E, Massault M, Michard G (2013) Carbon cycling and organic radiocarbon reservoir effect in a meromictic crater lake (Lac Pavin, Puy de Dôme, France). Radiocarbon 55(2):1029–1042

Anzidei M, Carapezza ML, Esposito A, Giordano G, Lelli M, Tarchini L (2008) The Albano Maar Lake high resolution bathymetry and dissolved CO_2 budget (Colli Albani volcano, Italy): constrains to hazard evaluation. J Volcanol Geotherm Res 171(3–4):258–268

Boivin P, Besson J-C, Briot D, Camus G, de Goër de Herve A, Gougaud A, Labazuy P, de Larouzière F-D, Livet M, Mergoil J, Miallier D, Morel J-M, Vernet G, Vincent P-M (2009) Volcanologie de la Chaîne des Puys, 4è édition bilingue, Editions du Parc Régional des Volcans d'Auvergne, Aydat, p 179

Boivin P, Besson JC, Ferry P, Gourgaud A, Miallier D, Thouret J-C, Vernet G (2012) Le point sur l'éruption du Lac Pavin, il y a 7000 ans. Actes du colloque international « Lac Pavin et autres lacs méromictiques », Besse-St-Anastaise, 14–16 mai 2009. Revue des Sciences Naturelles d'Auvergne 74–75, 2010–2011, 45–55

Bonhomme C, Poulin M, Vinçon-Leite B, Saad M, Groleau A, Jézéquel D, Tassin B (2011) Maintaining meromixis in Lake Pavin (Auvergne, France): the key role of a sublacustrine spring. Comptes Rendus Géosciences, Académie des Sciences 343(11):749–759

Boumehdi A (1988) Les clinopyroxènes dans les basaltes alcalins continentaux (Massif Central, France). Implications pétrogénétiques, barométriques et caractérisation de la profondeur des réservoirs magmatiques. Doctorat d'Université, Université Blaise Pascal - Clermont II, Clermont-Ferrand, 174 p

Bourdier J-L (1980) Contribution à l'étude volcanologique de deux secteurs d'intérêt géothermique dans le Mont Dore: le groupe holocène du Pavin et le massif du Sancy. Thèse, Université de Clermont II, 180 p

BRGM (2009) Evaluation préliminaire des conditions de stabilité des pentes du Lac Pavin. International Meeting "Lake Pavin and other meromictic lakes", Besse-St-Anastaise, 14–16 mai 2009. Service Aménagement et Risques naturels, DDE Puy de Dôme (Abstract p. x and unpublished presentation by O. Renaud 26 slides)

Brousse R (1961) Analyses chimiques des roches volcaniques du Tertiaire et Quaternaire de la France. Bulletin des Services de la carte géologique de la France et des topographies souterraines, 263, LVIII, 1–137

Bruyant C (1909) Le niveau du Pavin. In: Mélanges, 3è partie, Annales de la station limnologique de Besse, 203–205

Buettner R, Dellino P, La Volpe L, Lorenz V, Zimanowski B (2002) Thermohydraulic explosions in phreatomagmatic eruptions as evidenced by the comparison between pyroclasts and products from Molten Fuel Coolant Interaction experiments. J Geophys Res 107(B11):14–14

Büchel G (1993) Maars of the westeifel, Germany. In: Negendank, JFW, Zolitschka, B (eds) Paleolimnology of European maar lakes. Lecture notes in earth sciences, vol 49. Springer, pp 1–13

Büchel G, Lorenz V (1993) Syn-and post-eruptive mechanism of the Alaskan Ukinrek maars in 1977. In: Zolitschka B, Negendank JFW (eds) Paleolimnology of European Maar Lakes. Springer-Verlag, Berlin, pp 15–60

Camus G, Goër de Herve A de, Kieffer G, Mergoil J Vincent P-M (1973) Mise au point sur le dynamisme et la chronologie des volcans holocènes de la région de Besse-en-Chandesse (Massif Central francais). Copmptes-Rendus Académie des Sciences, Paris, 277(7): 629–632

Camus G, Michard G, Olive P, Boivin P, Desgranges P, Jézéquel D, Meybeck M, Peyrus J-C, Vincon JM, Viollier E, Kornprobst J (1993) Risques d'éruptions gazeuses carbonique en Auvergne. Bulletin Société géologique de France 164:767–781

Cas RAF, Wright JV (1987) Volcanic successions. Modern and ancient. Allen & Unwyn, London, p 519

Chapron E, Albéric P, Jézéquel D, Versteeg W, Bourdier J-L, Sitbon J (2010a) Multidisciplinary characterization of sedimentary processes in a recent maar lake (Lake Pavin, French Massif Central) and implication for natural hazards. Nat Hazards Earth Syst Sci 10:1–13

Chapron E, Alberic P, Jezequel D, Ledoux G and Massault M (2010b) Les archives sédimentaires de l'histoire du lac Pavin. Revue des Sciences Naturelles d'Auvergne, 74–75 (numéro spécial: Le lac Pavin), pp 57–66

Chapron E, Ledoux G, Simonneau A, Albéric P, St-Onge G, Lajeunesse P, Boivin P and Desmet M (2012) New evidence of Holocene mass wasting events in recent volcanic lakes from the French Massif Central (Lakes Pavin, Montcineyre and Chauvet) and implications for Natural Hazards. In: Yamada et al. (eds) Submarine mass move-

ments and their consequences, Advances in Natural and Technological Hazards Research 31, pp 255–264
Del Rosso-d'Hers T, Lavina P, Levi-Faict TW (2009) Risques naturels et péri-volcaniques du système volcanique Montchal-Pavin-Montcineyre. International meeting « Lake Pavin and other meromictic lakes », Besse en Chandesse, mai 2009, abstract p 72
Fox BRS, Wartho J, Wilson GS, Lee DE, Nelson FE, Kaulfuss U (2015) Long-term evolution of an Oligocene/Miocene maar lake from Otago, New Zealand. Geochem Geophys Geosyst 16(1):59–76
Freundt A, Strauch W, Kutterolf S, Schmincke HU (2007) Volcanogenic tsunamis in lakes: examples from Nicaragua and general implications. Pure Appl Geophys 164(2–3):527–545
Gal F, Gadalia A (2011) Soil gas measurements around the most recent volcanic system of metropolitan France (Lake Pavin, Massif central). Comptes Rendus Géosciences, Académie des Sciences 343:43–54
Gewelt M, Juvigné E (1988) Téphrochronologie du Tardiglaciaire et de l'Holocène dans le Cantal, le Cézallier et les Monts Dore (Massif Central, France): résultats nouveaux et synthèse. Bulletin de l'Association française pour l'étude du Quaternaire 25:25–34
Glangeaud P (1916) Le cratère-lac Pavin et le volcan de Montchalm (Puy-de-Dôme). Comptes Rendus Académie des Sciences Paris 162:428–430
Henriet JP (2009) Geophysical reconnaissance of Lac Pavin 2002. International meeting « Lake Pavin and other meromictic lakes », Besse en Chandesse, mai 2009, abstract p 29
Jézéquel D, Sarazin G, Fonty G, Tassin B (2008) Le Lac Pavin: le volcan, l'eau et la vie. Pour La Science, dossier n°58 « L'eau Attention fragile ! », janvier-mars 2008, pp 52–59
Jordan SC, Cas RAF, Hayman PC (2013) The origin of a large (>3 km) maar volcano by coalescence of multiple shallow craters: Lake Purrumbete maar, southeastern Australia. J Volcanol Geotherm Res 254:5–22
Juvigné E (1992a) Distribution of widespread late glacial and holocene tephra beds in the French Central Massif. Quat Int 14:181–185
Juvigné E (1992b) Approche de l'âge de deux cratères volcaniques lacustres d'Auvergne (France). Comptes Rendus Académie des Sciences, Paris 314:401–404
Lavina P (1985) Le volcan du Sancy et le « Massif Adventif » (Massif des Monts Dore, Massif Central Français). Etudes Volcanologiques et structurales. Thèse 3e cycle, Université de Clermont-Ferrand, 197 p
Lavina P and Del Rosso-d'Hers T (2008) Le complexe volcanique Montchal-Pavin-Montcineyre: nouvelles stratigraphie, teprochronologies et datations, vers une ré-évaluation de l'aléa volcano-tectonique en Auvergne. 22e Réunion des Sciences de la Terre, Nancy, France
Lavina P and Del Rosso-d'Hers T (2009) Le système volcanique du groupe Montchal-Pavin: nouvelle stratigraphie des formations volcano-sédimentaires et nouvelles datations, volcanologie dynamique, conséquences pour une évaluation des risques naturels. International meeting « Lake Pavin and other meromictic lakes », Besse en Chandesse, mai 2009, abstract p 15
Lavrieux M, Disnard J-R, Chapron E, Bréheret J-G, Jacob J, Miras Y, Reyss J-L, Andrieu-Pone V, Arnaud F (2013) 6700 yr sedimentary record of climatic and anthropogenic signals in Lake Aydat (French Massif Central). The Holocene 23(9):1317–1328
Lockwood JP, Costa JE, Tuttle ML, Nni J, Tebor SG (1988) The Potential For Catastrophic Dam Failure At Lake Nyos Maar, Cameroon. Bull Volcanol 50(5):340–349
Lorenz V (1973) On the formation of Maars. Bull Volcanol 37(2):183–204
Lorenz V (1986) On the growth of maars and diatremes and its relevance to the formation of tuff rings. Bull Volcanol 48:265–274
Lorenz V (1987) Phreatomagmatism and its relevance. Chem Geol 62(1–2):149–156
Lorenz V (2007) Syn- and posteruptive hazards of maar–diatreme volcanoes. J Volcanol Geotherm Res 159:285–312
Macaire J-J, Fourmont A, Argant J et al (2010) Quantitative analysis of climate versus human impact on sediment yield since the Lateglacial: the Sarlième palaeolake catchment (France). The Holocene 20(4):497–516
Németh K (2001) Long-term erosion-rate calculation from the Waipiata Volcanic Field (New Zealand) based on erosion remnants of scoria cones, tuff rings and maars. Géomorphologie: relief, processus, environnement 2:137–152
Németh K, Cronin SJ (2007) Syn- and post-eruptive erosion, gully formation, and morphological evolution of a tephra ring in a tropical climate erupted in 1913 in West Ambrym, Vanuatu. Geomorphology 86(1–2):115–130
Németh K, Kereszturi G (2015) Monogenetic volcanism: personal views and discussion. Int J Earth Sci 104(8):2131–2146
Németh K, Goth K, Martin U, Csillag G, Suhr P (2008) Reconstructing paleoenvironment, eruption mechanism and paleomorphology of the Pliocene Pula maar, (Hungary). J Volcanol Geotherm Res 177(2):441–456
Németh K, Cronin SJ, Smith IEM, Flores JA (2012) Amplified hazard of small-volume monogenetic eruptions due to environmental controls, Orakei Basin, Auckland Volcanic Field, New Zealand. Bull Volcanol 74(9):2121–2137
Olive P, Boulègue J (2004) Étude biogéochimique d'un lac méromictique: le lac Pavin, France. Géomorphologie: processus, relief, environnement 10(4):305–316
Ollier CD (1967) Maars. Their characteristics, varieties and definition. Bull Volcanol 31:45–73
Pirrung M, Büchel G, Lorenz V, Treutler H-C (2007) Post-eruptive development of the Ukinrek East Maar since its eruption in 1977 A.D. in the periglacial area of south-west Alaska. Sedimentology 55(2):305–334
Pirrung M, Buechel G, Merten D, Assing H, Schulte-Vieting U, Heublein S, Theune-Hobbs M, Boehrer B (2008) Morphometry, limnology, hydrology and sedimentology of maar lakes in East Java, Indonesia. Studia Quaternaria 21:139–152
Provencher L and Dubois J-M (2008) Proposition d'une nomenclature géomorphologique du ravage lacustre et comparaison avec les rivages côtiers et fluviaux. La société Provancher d'Histoire Naturelle du Canada, Université de Sherbrooke, pp 90–96
Rouwet D, Christenson B, Tassi F, Vandemeulebrouck J (eds) (2015) Volcanic lakes. advances in volcanology (Springer) ISBN 978-3-642-36832-5, 1–20
Schettler G, Schwab MJ, Stebich M (2007) A 700-year record of climate change based on geochemical and palynological data from varved sediments (Lac Pavin, France). Chem Geol 240:11–35
Schwab MJ, Schettler G, Bruchmann C, Acksel D, Negendank JFW, Brauer A (2009) Stratigraphy, chronology and paleoenvironment information of the sediment record from Lac Pavin, Massif Central (France). International Meeting-Lake Pavin and Other Meromictic Lakes, May 14–16, Besse et St-Anastaise, France, Abstract, p 30
Seib N, Kley J, Büchel G (2013) Identification of maars and similar volcanic landforms in the West Eifel Volcanic Field through image processing of DTM data: efficiency of different methods depending on preservation state. Int J Earth Sci 102(3):875–901
Stebich M, Brüchmann C, Kulbe T et al (2005) Vegetation history, human impact and climate change during the last 700 years recorded in annually laminated sediments of Lac Pavin, France. Rev Palaeobot Palynol 133:115–133
Suhr P, Goth K, Lorenz V, Suhr S (2006) Long lasting subsidence and deformation in and above maar-diatreme volcanoes – a never ending story. Z Dtsch Ges Geowiss 157(3):491–511
Tassi F, Rouwet D (2014) An overview of the structure, hazards, and methods of investigation of Nyos-type lakes from the geochemical perspective. J Limnol 73(1):55–70

Thouret J-C, Boivin P, Labazuy P, Leclerc A (2016) Geology, geomorphology and slope instability of the maar Lake Pavin (Auvergne, French Massif central). In: Lake Pavin. Springer, Cham

Touchart L (2000) Les lacs: origine et morphologie. L'Harmattan, Paris, 202 p

Vernet G (2013) La séquence sédimentaire des Gravanches/Gerzat: enregistrement d'événements catastrophiques à valeur chronologique en Limagne d'Auvergne (Massif Central, France). Quaternaire 24(2):109.127

Vespermann D, Schmincke HU (2000) Scoria cones and tuff rings. In: Sigurdsson et al (eds) Encyclopedia of volcanoes. Academic Press, pp 683–694

White J, Ross P-S (2011) Maar-diatreme volcanoes: a review. J Volcanol Geotherm Res 201:1–29

Wohletz K (1986) Explosive magma- water interactions: thermodynamics, explosions mechanisms, and field studies. Bull Volcanol 48:245–264